ORW controller displays a better noise attenuation than the LQRY controller.

Conclusions

The ORW control applied to two aeroelastic systems results in a better performance in terms of smoothness of response and decay time, but a greater sensitivity to process noise when compared to the traditional output-weighted optimal control. Its use may lie in controlling well-modeled plants where robustness is less critical, but where smoothness of response is important for issues such as passenger comfort, or weapons aiming and delivery.

References

[1]Friedland, B., *Control System Design: An Introduction to State-Space Methods*, McGraw–Hill, New York,1987, pp. 364–365.

[2]Stein, G., and Athans, M., "The LQG/LTR Procedure for Multivariable Feedback Control Design,"*IEEE Transactions on Automatic Control*, Vol. 32, 1987, pp. 105–114.

[3]Linz, S. J., "Nonlinear Dynamical Models and Jerky Motion," *American Journal of Physics*, Vol. 65, No. 6, 1997, pp. 523–526.

[4]Zhou, K., and Doyle, J. C., *Essentials of Robust Control*, Prentice–Hall, Upper Saddle River, NJ, 1998, p. 254.

[5]Newman, B., and Schmidt, D. K., "Numerical and Literal Aeroelastic Vehicle Model Reduction for Feedback Control Synthesis," *Journal of Guidance, Control, and Dynamics*, Vol. 14, No. 5, 1991, pp. 943–953.

[6]Waszak, M., and Schmidt, D. K., "Flight Dynamics of Aeroelastic Vehicles," *Journal of Aircraft*, Vol. 25, No. 6, 1988, pp. 563–571.

[7]Tewari, A., "Output Rate Weighted Active Flutter Suppression," AIAA Paper 99-4312, Aug. 1999.

Measurement Rate Reduction in Hybrid Systems

D. D. Sworder*
University of California,
San Diego, La Jolla, California 92037
and
J. E. Boyd†
Cubic Defense Systems, San Diego, California 92186

I. Introduction

In some tracking applications, location estimates are found by first approximating the conditional distribution of the state vector with a Gaussian sum distribution. Gaussian sums have proven their worth in various problems, particularly those with hybrid dynamic models.[1] However, in an encounter involving multiple aircraft, tracked with multiple sensors, and having multiple motion modes, the number of possible hypotheses delineating the temporal evolution of the motion/observation path grows geometrically. If each modal path is associated with an element in a Gaussian sum, the comprehensive conditional density has too many terms. The geometric growth in complexity forces a designer to simplify the distribution through a process of mixture reduction. Several plausible methods of avoiding hypothesis bloating are provided in Ref. 2.

In this Note, the focus is on a single target that is maneuvering in the plane. The maneuver path is created by changing the motion mode of the aircraft, for example, coasting, turning, jinking, and so on. If the modal path were known, conventional methods could be used to estimate the state of the target. However, the unpredictable (and unmeasured) modal dynamics create considerable difficulty.

Received 7 April 2000; revision received 4 September 2000; accepted for publication 16 October 2000.

*Professor, Department of Electrical and Computer Engineering, 9300 Gilman; dsworder@ucsd.edu.

†Chief Scientist, P.O. Box 85587; john.boyd@cubic.com.

To be more specific, suppose the motion model of the target is defined on a particular probability space and the time interval $[0, T]$. There are two right-continuous, random processes: $\{\Phi_t\}$, a piecewise constant modal process ranging over an index set of size $\boldsymbol{S}$, and $\{\boldsymbol{w}_t\}$, a Brownian motion. The modal state $\boldsymbol{\phi}_t$ is a unit vector in $\mathbb{R}^S$ with state space $\{\boldsymbol{e}_1, \ldots, \boldsymbol{e}_S\}$. The component in $\boldsymbol{\phi}_t$ with value one marks the current motion mode. The modal dynamics are usually represented by an exogenous Markov model with generator Q'. For notational convenience in what follows, $\boldsymbol{e}_i$ is the ith canonical unit vector in a space whose dimension is obvious from the context. Where no confusion will arise, a subscript may identify time, the component of a vector, or the element of an indexed family with the meaning determined by context; similarly a superscript may denote a power operator or an element of an indexed family. If a process is sampled, the discrete sequence so generated is written $\{\boldsymbol{y}[k]\}$, where the index denotes sample number rather than time. Conditional expectation is denoted with a circumflex, with the relevant σ field apparent from context. A Gaussian random variable with mean $\hat{\boldsymbol{x}}_t$ and covariance P_{xx} is indicated by $\boldsymbol{x} \sim \boldsymbol{N}(\hat{\boldsymbol{x}}_t, \boldsymbol{P}_{xx})$ with the same symbol used for the density function itself where no confusion will arise. If A is a positive symmetric matrix and $\boldsymbol{x}$ a compatible vector, $\boldsymbol{x}'A\boldsymbol{x}$ is denoted $\|\boldsymbol{x}\|_A^2$. Denote the inverse of a (positive) covariance matrix, P, by D; for example, $D_i = (P_i)^{-1}$. If $\boldsymbol{m}$ is a vector of conditional means, the product $D\boldsymbol{m}$ is denoted $\boldsymbol{d}$, for example, $\boldsymbol{d}_i = D_i\boldsymbol{m}_i$.

Both time-continuous and time-discrete models have been used in tracking applications, the latter formed by sampling the relevant variables of the former. The linear, time-discrete hybrid model can be derived from the time-continuous model as in Ref. 1:

$$\boldsymbol{x}[k] = \sum_i (A_i\boldsymbol{x}[k-1] + C_i\boldsymbol{w}[k])\boldsymbol{\phi}_i[k-1] \tag{1}$$

$$\boldsymbol{\phi}[k] = \Pi\boldsymbol{\phi}[k-1] + \boldsymbol{m}[k] \tag{2}$$

where $\{\boldsymbol{w}[k]\}$ is a unit Gaussian white sequence and $\{\boldsymbol{m}[k]\}$ is a martingale increment sequence. The vector $\boldsymbol{x}[k]$ is called the base state to distinguish it from the modal state. The modal transition matrix Π can be computed from Q in the customary way. If the time-continuous models are controllable from the plant noise process in every regime, C_i and A_i are both nonsingular for all i. Label the local plant-noise covariance by $R_\chi(i) > 0$.

In common applications, a sensor gives a linear (or linearizable) measurement of the base-state vector:

$$\boldsymbol{y}[k] = H\boldsymbol{x}[k] + \boldsymbol{n}[k] \tag{3}$$

where $\{\boldsymbol{n}[k]\}$ is a Gaussian white sequence with positive covariance R_x. The measurement rate is determined by the sensor and its utilization policy. The measurements may occur at a different rate than the basic clock rate, usually much slower, and the sensor gain can be made time dependent so that at times of no measurement the observation is uninformative.

The initial plant-state categories are assumed to be independent with probability distributions $\boldsymbol{x}[0] \sim \boldsymbol{N}(\hat{\boldsymbol{x}}[\boldsymbol{0}], \boldsymbol{P}_{xx}[\boldsymbol{0}])$ and $\boldsymbol{\phi}[0] \sim \hat{\boldsymbol{\phi}}[0]$. Denote the filtration generated by the measurements by $\mathcal{G}[k]$. The basic tracking problem is that of estimating $\boldsymbol{x}[k]$ on the basis of $\mathcal{G}[k]$.

Investigators have studied hybrid-state estimation with an emphasis on time-continuous plants and a mix of time-continuous and time-discrete observations. The polymorphic estimator (PME) is a practical algorithm for approximating the $\mathcal{G}_t$-regime probabilities along with those $\mathcal{G}_t$ moments important in path following.[1] The PME is moment based and does not provide the $\mathcal{G}_t$-distribution function of the hybrid state.

The motion model is a hybrid in which the kinematics are represented in the conventional manner, and the mode is represented by a random regime process. Good location estimates are produced at reasonable computational cost by algorithms that approximate the conditional density of the kinematic state using an S-fold Gaussian sum; these are also called path-length-one algorithms because they look back one step in the evolution of the modal process:

$$q[k] = \sum_{l=1}^{S} \alpha_l[k]\boldsymbol{N}(\boldsymbol{m}_l[k], \boldsymbol{P}_l[k]) \tag{4}$$

In a parallel effort, the reference probability method was used to develop the Gaussian wavelet estimator (GWE) (see Refs. 3 and 4). When the trajectory discontinuities and the measurement biases that give the GWE its special character are neglected, a path-length-two version of the GWE (looking back two steps) would be

$$q[k] = \sum_{i,j,l=1}^{S} \alpha^i_{jl}[k] \boldsymbol{N}\big(\boldsymbol{m}^j_l[k], \boldsymbol{P}^j_l[k]\big) \tag{5}$$

Equations (4) and (5) and the distributions that follow will be written in either their normalized

$$\sum_l \alpha_l = 1$$

or equivalently, in their unnormalized

$$\sum_l \alpha_l \neq 1$$

form without comment. The coefficients $\{\alpha_l[k]\}$ are viewed as the conditional probabilities of the modal states $\phi[k]$, and the Gaussian primitives are viewed as the conditional densities of the base state given the current modal state. Equation (4) has been used both when the modes do not communicate [the multiple model adaptive estimator (MMAE)[5]] and when they do [the interacting multiple model estimator (IMM)[6]]. The IMM is particularly effective because it uses a sophisticated merging step to convert a path-length-one algorithm to one with performance approaching the path-length-two algorithm.

The GWE has much in common with the IMM, for example, a bank of parallel Kalman filters. However, the hypothesis-merging step in the GWE is considerably different. In contrast to the IMM and the MMAE, the GWE requires pruning to maintain a fixed number of terms in the distribution. It is the objective of this Note to show that the increased complexity is justified in applications in which the observation rate is low. When the observation rate is high, the simpler algorithms perform as well and are easier to implement.

II. Multiple Model Estimators

The distribution-based, time-discrete, estimation problem can be posed as follows. Suppose that at time $t = kT$ the $\mathcal{G}[k]$ density of the hybrid state is approximated by Eq. (5) [or its analog, Eq. (4)]. The fundamental mapping is that from $(\alpha^i_{jl}[k], \boldsymbol{m}^j_l[k], P^j_l[k], \boldsymbol{y}[k+1])$ to $(\alpha^i_{jl}[k+1], \boldsymbol{m}^j_l[k+1], P^j_l[k+1])$. When certain discontinuities and biases are absent, the recurrence formula for the unnormalized conditional density of the hybrid state can be derived using the reference probability approach.[1] To avoid geometric growth in the number of terms, a mixture reduction step is required. The path-length-two reduction to Eq. (5) is presented in Ref. 7.

The GWE can be most concisely stated in a mixed covariance-information form.[8] The information matrix is the inverse of the covariance matrix, and instead of framing the estimator using $\{m_l\}$ and $\{P_l\}$ as coordinates, the information filter also propagates $\{d_l\}$ and $\{D_l\}$. Denote the matrix form $P^{ijl}_{yy} = R_x + H' P^{i-}_{jl} H$. Then, for GWE recurrence, extrapolate $i, j, l \in \boldsymbol{S}$,

$$\boldsymbol{m}^{i-}_{jl}[k+1] = A_i \boldsymbol{m}^j_l[k] \tag{6}$$

$$P^{i-}_{jl}[k+1] = A_i P^j_l[k] A'_i + R_\chi(i) \tag{7}$$

and update $i, j, l \in \boldsymbol{S}$,

$$\Delta \boldsymbol{d}^{i+}_{jl}[k+1] = H' D_x \boldsymbol{y}[k+1] \tag{8}$$

$$\Delta D^{i+}_{jl}[k+1] = H' D_x H \tag{9}$$

where $\Delta \boldsymbol{d}^{i+}_{jl}[k+1] = \boldsymbol{d}^{i+}_{jl}[k+1] - \boldsymbol{d}^{i-}_{jl}[k+1]$ (similarly $\Delta D^{i+}_{jl}[k+1]$). Define

$$L^i_{jl} = \left| D^{ijl}_{yy}[k+1] \right|^{-\frac{1}{2}} \exp \tfrac{1}{2} \Delta \left\| \boldsymbol{m}^{i+}_{jl}[k+1] \right\|^2_{D^{i+}_{jl}[k+1]}$$

The weighting coefficients in the GWE satisfy the following. For GWE modal recurrence, update, for $i, j, l \in \boldsymbol{S}$,

$$\alpha^{i-}_{jl}[k+1] = L^i_{jl} \alpha^i_{jl}[k+1] \tag{10}$$

Transition, for $p, i, j, l \in \boldsymbol{S}$,

$$\alpha^{pi}_{jl}[k+1] = \Pi_{pi} \alpha^{i-}_{jl}[k+1] \tag{11}$$

Before the iteration is complete, mixture reduction is needed. In Ref. 2, densities are merged on the basis of their size and distance from the principal components. In the GWE, mixture reduction is achieved by retaining a single element from each path of length two preceding the current modal state using the conventional Gaussian sum merging formula. As a notational convenience, denote the normalized family of α^{pi}_{jl} (or similar families) by $\bar{\alpha}^{pi}_{jl}$. The mixture reduction formula is

$$\alpha^i_{jl}[k+1] = \sum_{p=1}^{S} \bar{\alpha}^{ij}_{lp}[k+1], \qquad \boldsymbol{m}^i_j[k+1] = \sum_{l=1}^{S} \boldsymbol{m}^{i+}_{jl}[k+1] \bar{\alpha}^{i-}_{jl} \tag{12}$$

$$P^i_j[k+1] = \sum_{l=1}^{S} \left(P^{i+}_{jl}[k+1] + \left(\boldsymbol{m}^{i+}_{jl}[k+1] - \boldsymbol{m}^i_j[k+1] \right)(\cdot)' \right) \bar{\alpha}^{i-}_{jl} \tag{13}$$

The recurrence of the GWE estimator is complete, and the various moments of interest can be computed in the conventional manner.

The IMM has a similar form but begins with a less differentiated Gaussian sum. As was the case in the GWE, extrapolation update in the IMM utilizes a set of S Kalman filters. The filters are initialized with $\{\boldsymbol{m}_l[k], P_l[k]; l \in \boldsymbol{S}\}$, and after an observation, each generates a residual, $\boldsymbol{r}_l[k+1] = \boldsymbol{y}[k+1] - H\boldsymbol{m}_l[k+1]^-$ with pseudocovariance $P^l_{yy}[k+1]$. The IMM (and the MMAE) employs the residuals to update the modal estimate (Ref. 9). Let $M_l = |D^l_{yy}[k+1]|^{1/2} \exp -\frac{1}{2} \|\boldsymbol{r}_l[k+1]\|^2_{D^l_{yy}[k+1]}$. Then, for IMM modal recurrence, update, for $l \in \boldsymbol{S}$,

$$\alpha^-_l[k+1] = M_l \alpha_l[k+1] \tag{14}$$

Transition, for $p, l \in \boldsymbol{S}$,

$$\alpha_l[k+1] = \sum_{p=1}^{S} \Pi_{lp} \alpha^-_p[k+1] \tag{15}$$

The IMM does not require mixture reduction to maintain the correct number of hypotheses. Merging after a measurement is, however, required for good performance, and the required formulas are given in the references.

The IMM and the GWE perform common operations on the data. Both algorithms require S Kalman filters, but in the GWE, each filter extrapolates more initial conditions. The fundamental difference between the algorithms arises from the way they utilize the observation to improve modal estimation. Each filter in the IMM generates a residual. The bigger this residual is, normalized by the information matrix $D^l_{yy}[k+1]$, the smaller is the factor that multiplies the a posteriori mode probability. This is plausible because an incorrect filter will have a large, and probably biased, residual for the most part. The GWE adjusts the modal probabilities in a different way, emphasizing hypotheses that maximize the normalized change in the magnitude of $\boldsymbol{m}^i_{jl}$. This does not have the intuitive appeal of residual minimization, but as will be seen, it is quite effective in certain situations.

III. Path-Following Example

Measurement sample rates for target tracking vary according to the application, and in some cases they are relatively slow; for example, in air traffic control, the interval between samples may be 5 s (the ASR-9 air traffic control surveillance radar[10]). In other applications, the sample rates are intentionally reduced to the degree possible. In sessions devoted to tracking maneuvering targets using a phased array radar at the 1994 and the 1995 American Control

Conference meetings, the performance metric used was "minimization of the number of radar dwells" while satisfying a constraint on loss of track.[11] In such applications, an engineer seeks to determine the minimum measurement rate required for satisfactory path-following performance.

To illustrate, consider an aircraft maneuvering at nearly constant altitude and speed, for example, in the XY plane. A simple, kinematic equation can be used to delineate the motion:

$$\mathrm{d}\begin{bmatrix} V_x \\ V_y \end{bmatrix} = \begin{bmatrix} 0 & -\Phi \\ \Phi & 0 \end{bmatrix}\begin{bmatrix} V_x \\ V_y \end{bmatrix}\mathrm{d}t + \begin{bmatrix} 1 & 0 \\ 0 & 1 \end{bmatrix}\mathrm{d}\begin{bmatrix} w_x \\ w_y \end{bmatrix} \qquad (16)$$

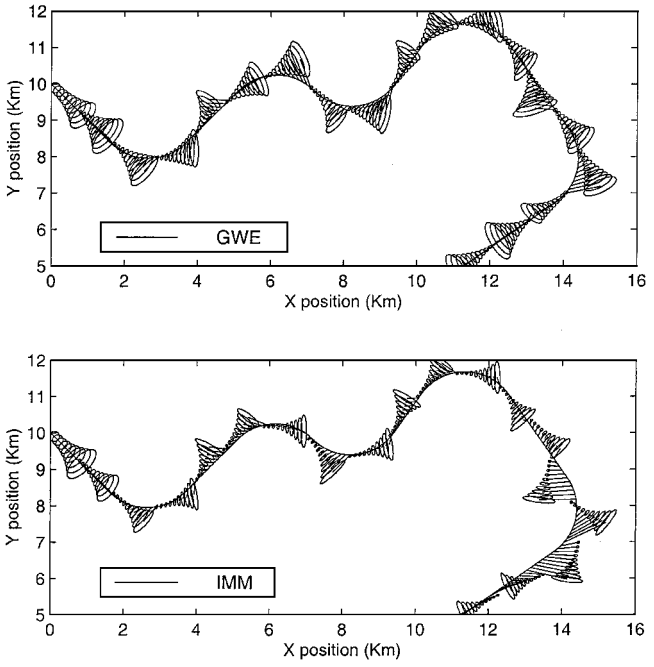

Fig. 1 Tracking the path of the target using radar 2, T = 5 s.

The kinematic state consists of the velocity vector (V_x, V_y) and its integral, the position vector (X, Y). The primary forcing function is the maneuver turn rate $\{\Phi_t\}$, and there is also a small wideband acceleration $\{\boldsymbol{w}_t\}$ of intensity $W_0\boldsymbol{I}t = E[\boldsymbol{w}_t\boldsymbol{w}_t']$ to account for a variety of high-frequency effects.

To contrast the performance of estimators of varying complexity, we will track the target using a location sensor (a radar) located at the origin of the coordinate system with noise that is additive and uncorrelated (in space and time), zero mean, and Gaussian. Radar 1 has a 1-σ range error of 20 m and a bearing error of 4 mr (40-m cross range at 10 km). Radar 2 has a 1-σ range error of 40 m and bearing error 2 mr. These radars are of good quality: Compare the 100-m Cartesian error in both directions in Ref. 12 (with correlation between components) and Ref. 10 and the 110-m range and 3.5 mr bearing error in Ref. 13.

The sensor can operate with intersample period T in the interval [1, 9] s. This range covers the ATC application and that found in Ref. 13 ($T = 4.5$ s). The sample rate is greater than that used in Ref. 12 ($T = 10$ s) because of the agility of the target. The intensity of the local target acceleration is $W_0 = 0.2$; greater than $W_0 = 0$ in Ref. 12 and $W_0 = 10^{-6}$ in Ref. 10 but not enough to stabilize the IMM in all circumstances.

The target follows a path created by coasts and left or right turns at rate 10 deg/s. A Markov maneuver model can be produced for the target using conventional methods. The initial conditions for the estimators are as follows. Coast mode is favored initially, with the initial standard deviation in location equal to 100 m and velocity equal to 22 m/s. The sample interval used to discretize the time-continuous model is 0.5 s, and for convenience, each of the estimators is initialized at the initial target state.

A sample path showing the response of the GWE and the IMM when radar 2 is used is shown in Fig. 1 for $T = 5$ s. The path is generated without wideband accelerations, and the trackers receive identical observations. The target is detected at $(\boldsymbol{X}_0, \boldsymbol{Y}_0) = (0, 10)$ km, moving with a velocity of $(\boldsymbol{V}_{x0}, \boldsymbol{V}_{y0}) = (0.2, -0.2)$ km/s. The path of the aircraft is the continuous curve. An error ellipse (from the computed covariance) of size 1.4σ is centered on the mean estimate and displayed every 0.5 s. It is evident that, following an update, the location estimates from the algorithms tend to be close to the target and close to each other. The GWE ellipses enclose the path with one

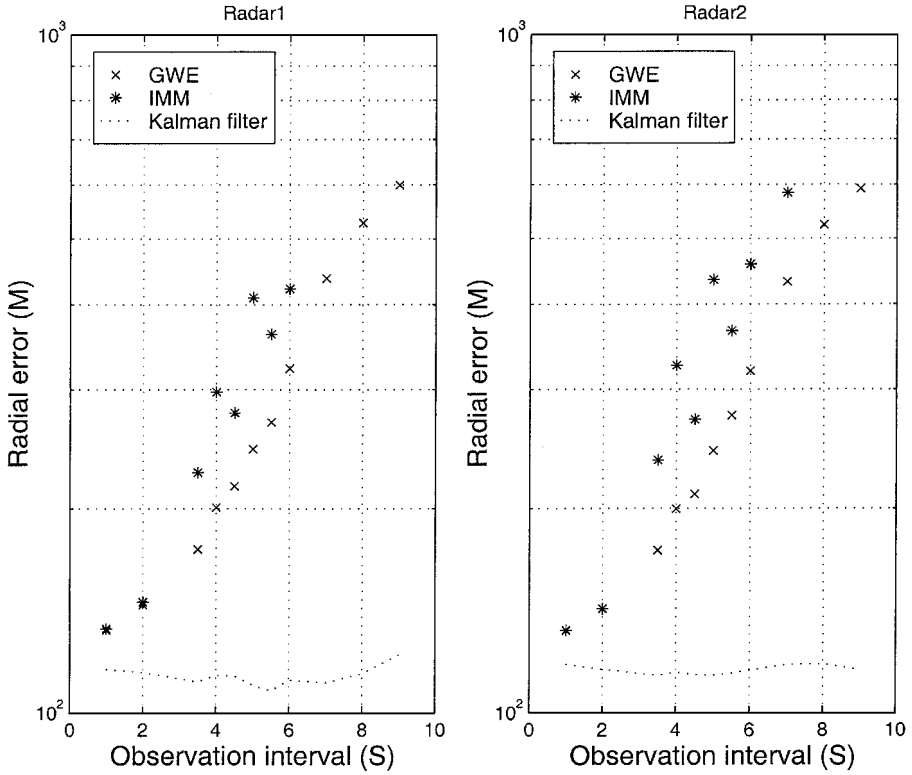

Fig. 2 Mean radial tracking error: radars 1 and 2.

significant exception in the last turn. The IMM generates smaller ellipses. This makes following the last turn more problematic because of the ambiguity inherent in the measurement residuals.

To quantify the relative performance of the trackers better, 50 independent observation sequences were generated for several measurement rates. The same measurement sequences were used as the input to each algorithm, and the results were time and ensemble averaged. Figure 2 shows mean radial tracking error for each radar. The GWE and the IMM are shown along with the performance of a path-adapted Kalman filter that provides a (unrealizable) lower bound. For fast samplers (less than 3 s), the GWE conveys little benefit. As the intersample interval increases, modal identification becomes more important, and the GWE becomes the algorithm of choice. In this low plant-noise environment, the Kalman filter is relatively insensitive to sample rate: The radial error is approximately 120 m.

Above sample intervals of $T = 3$ s, the GWE achieves the performance of the IMM with a sample interval about 1 s slower. The IMM has some sample rate resonances at low rates. At rates below 0.17 Hz, the IMM generates singular sample covariances on some sample paths. When this occurs, the mean radial error is not plotted in Fig. 2. The IMM can be stabilized by adding pseudonoise (as is done in the extended Kalman filter in Ref. 14) at the expense of an increase in the size of the error ellipses. This was not done here; all algorithms used the same encounter parameters and the same observation data.

IV. Conclusions

High-quality estimation of a dynamic hybrid system requires careful mixture reduction. Performance is not always commensurate with complexity. The GWE and the IMM differ little when the intermeasurement time is small. At long intermeasurement intervals, the GWE is the algorithm of choice.

References

[1]Sworder, D. D., and Boyd, J. E., *Estimation Problems in Hybrid Systems*, Cambridge Univ. Press, New York, 1999, pp. 197–220.

[2]Pao, L. Y., "Multisensor Multitarget Mixture Reduction Algorithms for Tracking," *Journal of Guidance, Control, and Dynamics*, Vol. 17, No. 6, 1994, pp. 1205–1211.

[3]Sworder, D. D., Boyd, J. E., and Elliott, R. J., "Modal Estimation in Hybrid Systems," *Journal of Mathematical Analysis and Applications*, Vol. 245, No. 3, 2000, pp. 225–247.

[4]Leondes, C. T., Sworder, D. D., and Boyd, J. E., "Multiple Model Methods in Path Following," *Journal of Mathematical Analysis and Applications* (to be published).

[5]Vasquez, J. R., and Maybeck, P. S., "Density Algorithm Based Moving-Bank MMAE," *Proceedings of the Conference on Decision and Control*, IEEE Publications, Piscataway, NJ, 1999, pp. 4117–4122.

[6]Mazor, E., Averbuch, A., Bar-Shalom, Y., and Dayan, J., "Interacting Multiple Model Methods in Target Tracking: A Survey," *IEEE Transactions on Aerospace and Electronic Systems*, Vol. 34, No. 1, 1998, pp. 103–123.

[7]Sworder, D. D., and Boyd, J. E., "A New Merging Formula for Multiple Model Trackers," *Proceedings of the SPIE: Signal and Data Processing of Small Targets*, Vol. 4048, SPIE Publications, Orlando, FL, 2000, pp. 498–509.

[8]Elliott, R. J., Aggoun, L., and Moore, J. B., *Hidden Markov Models: Estimation and Control*, Springer-Verlag, New York, 1995, p.100.

[9]Li, X. R., "Engineers' Guide to Variable-Structure Multiple-Model Estimation for Tracking," *Multitarget-Multisensor Tracking: Advances and Applications*, Vol. 3, 2000 (to be published).

[10]Li, X. R., and Bar-Shalom, Y., "Design of an Interacting Multiple Model Algorithm for Air Traffic Control Tracking," *IEEE Transactions on Control Systems Technology*, Vol. 1, No. 3, 1993, pp. 186–194.

[11]Blair, W. D., Watson, G. A., and Hoffman, S. A., "Benchmark Problem for Beam Pointing Control of Phased Array Radar Against Maneuvering Targets," *Proceedings of the American Control Conference*, IEEE Publications, Piscataway, NJ, 1994, pp. 2071–2075.

[12]Cloutier, J. R., Lin, C. F., and Yang, C., "Enhanced Variable Dimension Filter for Maneuvering Target Tracking," *IEEE Transactions on Aerospace and Electronic Systems*, Vol. 29, No. 3, 1993, pp. 786–797.

[13]Helmick, R. E., Blair, W. D., and Hoffman, S. A., "Interacting Multiple-Model Approach to Fixed Interval Smoothing," *Proceedings of the Conference on Decision and Control*, IEEE Publications, Piscataway, NJ, 1993, pp. 100–106.

[14]Mook, J. D., and Shyu, I. M., "Nonlinear Aircraft Tracking Filter Utilizing Control Variable Estimation," *Journal of Guidance, Control, and Dynamics*, Vol. 15, No. 1, 1992, pp. 228–237.